An OFDM Testbed for LiFi Performance Characterization of Photovoltaic Modules

1st N. Lorrière
Aix Marseille Univ, Univ Toulon, CNRS, IM2NP
Marseille, France
nominoe.lorriere@im2np.fr

2nd E. Bialic
Sunpartner Technologies
Rousset, France
ebialic@sunpartner.fr

3rd M. Pasquinelli
Aix Marseille Univ, Univ Toulon, CNRS, IM2NP
Marseille, France
marcel.pasquinelli@univ-amu.fr

4th G. Chabriel
Univ Toulon, Aix Marseille Univ, CNRS, IM2NP
La Garde, France
gilles.chabriel@univ-tln.fr

5th J. Barrère
Univ Toulon, Aix Marseille Univ, CNRS, IM2NP
La Garde, France
jean.barrere@univ-tln.fr

6th L. Escoubas
Aix Marseille Univ, Univ Toulon, CNRS, IM2NP
Marseille, France
Ludovic.escoubas@univ-amu.fr

7th J.-J. Simon
Aix Marseille Univ, Univ Toulon, CNRS, IM2NP
Marseille, France
jean-jacques.simon@univ-amu.fr

***Abstract*—OFDM-based wireless communications are widely used for digital data RF transmissions. This very efficient modulation scheme should prove to be one of the solutions for future VLC (visible light communications) systems. Moreover, for outdoor applications, photovoltaic modules seem to be interesting alternatives to photodiode-based classical detectors. They are indeed known to offer a higher level of resilience to saturation effects. In this article, we present LiFi performance results obtained from an OFDM-based LiFi testbed using various photovoltaic modules as photodetectors.**

***Index Terms*—LiFi, Visible Light Communication (VLC), DC biased Optical - Orthogonal Frequency Division Multiplexing (DCO-OFDM), PV receiver, Semi-transparent Photovoltaic Module, I(V), impedance spectroscopy, indoor/outdoor applications**

I. Introduction

LiFi technology uses LED light bulbs as emission source to carry numerical data from visible light high-frequency modulations (see e.g. [3] for a complete survey in french). Classically, at the reception end, a conventional photodiode converts the light intensity variations (imperceptible to the human eye) into an electrical signal, which is later decoded by a LiFi soft demodulator. There are two major drawbacks regarding the use of a photodiode for LiFi roaming applications: first, this type of receiver needs to be powered and second, it becomes saturated in outdoor conditions. PV modules would be suitable candidates to replace photodiodes: thanks to their large surface, PV modules have sufficient intern built-in voltage for separating electron-hole pairs in the depletion region. Moreover, it has been demonstrated that solar cells can improve LiFi in reliability in outdoor environment due to a lower saturation level compared to standard photodiodes [1]. In this work, we first focus on the description of the particular LiFi test bench we developed. In the next section III, test measurements are compared with those obtained by Bialic *et al* [4] from a close LiFi test bench. Finally, very first results obtained from various semi-transparent photovoltaic modules developed by Sunpartner Technologies are presented in section IV.

Work made in collaboration with Aix-Marseille University, Toulon University and Sunpartner Technologies company.

II. Measure of LiFi performance

In order to assess performance of various LiFi hardwares –the emitting LED and/or the receiving photovoltaic (PV) module–, we developed a versatile LiFi test bench. Testing being conducted in real conditions of use, the objective is to simultaneously give several performance indicators as e.g. frequency responses in terms of complex magnitude, signal-to-noise ratio (SNR) and bit error rate (BER). To provide such real conditions frequency behaviors, the CP-OFDM (cyclic prefix - orthogonal frequency division multiplexing) modulation scheme appears to be the most appropriate, both allowing data efficient transmission [2], [3] and frequency channel simplified characterization [1].

A. General overview of our LiFi Test Bench

Our platform of experimentation (see Fig. 1) involves a personal computer (PC) enabling to both control LiFi transmission and reception from a man-machine interface (MMI) using Matlab (see Fig. 2).
At the emission, the software generates a set of oversampled CP-OFDM digital symbols that is sent to an arbitrary function

generator (AFG) via an USB link. The AFG converts the OFDM digital symbols into a voltage signal for modulating the intensity of the LED lighting. When high power LEDs are used, the system may support an additional current generator. The AFG output and the current generator being connected to the LED using a bias tee.
On the receiver's side, the photovoltaic module is connected directly to a digital oscilloscope that samples the open-circuit voltage (Voc) signal at the OFDM sample period. The samples are returned to the PC via an USB link in order to be saved then postprocessed with the MMI.

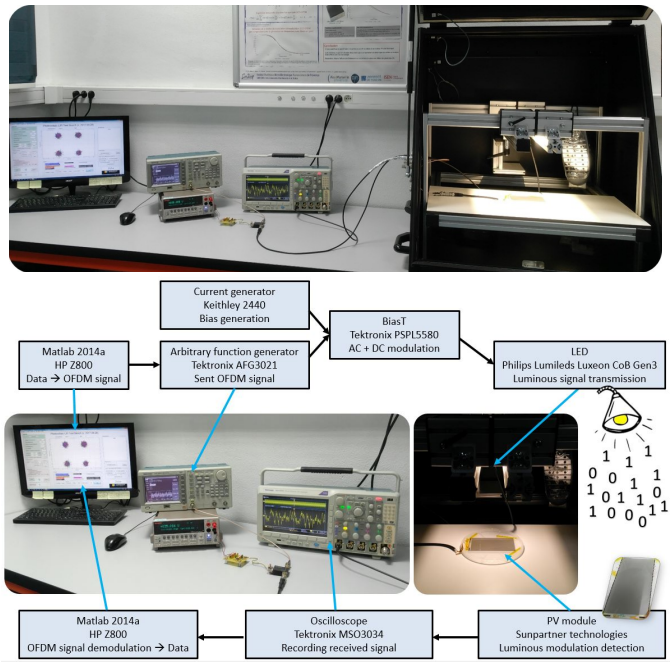

Fig. 1. IM2NP's LiFi testbed

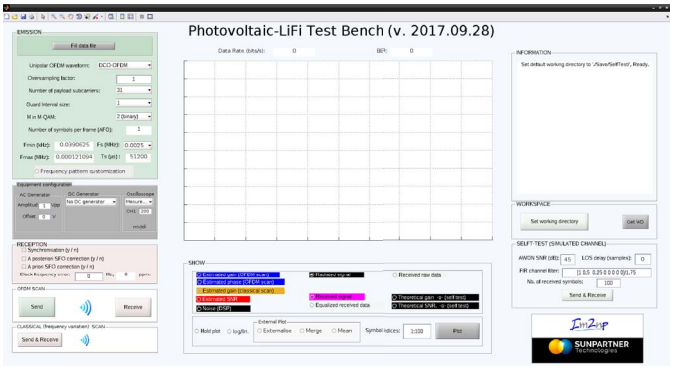

Fig. 2. LIFI testbed's Matlab IHM

B. DCO-OFDM modulation/demodulation scheme

The first OFDM modulation schemes [4] were widely adapted to digital wideband transmissions such as digital video broadcasting - terrestrial (DVB-T), audio broadcasting [6], DSL internet access, etc. and now optical communications [7]. OFDM is a particular method of multi-carrier amplitude modulation where the different carriers are chosen to be orthogonal two by two (in the usual scalar product sense) on a given time duration. Beside its high spectral efficiency due to the optimal carrier frequency spacing, the CP-OFDM modulation scheme allows to simplify the equalization process assuming a finite impulse response (FIR) linear transmission channel preserving the orthogonality between carriers in order to prevent interference between data due to crosstalk.
Originally, the OFDM baseband signal is both complex and bipolar. Such a signal is adapted to IQ RF communications but not to LiFi since light intensity modulations require real and positive modulating signals. One suitable variant of the OFDM modulation scheme is the so called DC-biased Optical CP-OFDM (DCO-CP-OFDM) about which we would like to recall its main characteristics.

1) DCO-CP-OFDM symbol structure: In the LiFi testedbed, the PC aims to send to the AFG the zero-mean version (hence bipolar) of the DCO-CP-OFDM digital signal. The DC component being later added either directly by the AFG or analogically by the current generator depending on the power of the emitting LED. The DCO-CP-OFDM digital signal is a sequence of OFDM symbols $s^m[n]$, with $2K+L$ real samples each. Any m^{th} OFDM symbol represents the sampled version of a modulated signal of finite duration corresponding to the IQ amplitude modulation of $K-1$ carrier waveforms by $K-1$ complex data d_k^m from a QAM finite alphabet. The real part of any datum d_k^m modulates the "In-phase" component of the carrier waveform k while the imaginary part is applied to its "Quadrature" component. To ensure the symbol is real, it can be shown that at least $2K$ samples are required: $2(K-1) = 2K-2$ samples to obtain a conjugate symmetrical (Hermitian) discrete spectra, one additional sample for the mean value and a last sample so that the total number of samples is even to allow an efficient construction with fast Fourier transform (FFT) algorithm. Now, using L additional samples for the cyclic prefix, one has:

$$s^m[n] = \frac{1}{K}\sum_{k=1}^{K-1} \mathsf{Re}(d_k^m)\cos\left(2\pi\frac{kn}{2K}\right) - \mathsf{Im}(d_k^m)\sin\left(2\pi\frac{kn}{2K}\right),$$
$$n \in \{-L,\ldots,2K-1\}.$$

The previous expression can be rewritten in a more compact form using complex notation:

$$s^m[n] = \frac{1}{2K}\sum_{k=0}^{2K-1} S^m[k]\exp\left(\mathrm{j}2\pi\frac{kn}{2K}\right),$$
$$n \in \{-L,\ldots,2K-1\}, \qquad (1)$$

where $S^m[k] = d_k^m$ and $S^m[2K-k] = (d_k^m)^*, k \in \{1,\ldots,K-1\}$ and where $S^m[0] = S^m[K] = 0$. This last set of equalities both ensuring a zero-mean value and the

Hermitian symmetry. It can be noticed that the orthogonality between the carrier waveforms is satisfied:

$$\frac{1}{2K}\sum_{n=0}^{2K-1}\exp\Big(\mathrm{j}2\pi\frac{kn}{2K}\Big)\exp\Big(-\mathrm{j}2\pi\frac{k'n}{2K}\Big)=\delta_{kk'}, \quad (2)$$

where $\delta_{kk'}$ denotes the Kronecker symbol.
The temporal sequence $s^m[n], n \in \{0,\dots,2K-1\}$ corresponds to the inverse discrete Fourier transform of the frequential sequence $S^m[k], k \in \{0,\dots,2K-1\}$. It can then be efficiently computed using FFT if $2K$ is chosen as a power of 2. The remaining L first samples $s^m[n], n \in \{-L,\dots,-1\}$ corresponding to the cyclic prefix are obtained by periodical extension *i.e.* taking the L last samples $s^m[n], n \in \{2K-L,\dots,2K-1\}$.
Now, from, the sequence of samples $s^m[n], n \in \{-L,\dots,2K-1\}, m \in \{1,\dots,M\}$, the AFG produces a DC-biased voltage signal by digital-to-analog conversion (DAC) with a F_s update rate.
Due to the necessary limited slope of the AFG's restitution low-pass filter, such a signal would exhibit a frequency range significantly wider than the expected one *i.e.* $\left[\frac{F_s}{2K}, \frac{F_s}{2}-\frac{F_s}{2K}\right]$. In particular, the maximal frequency can exceed the Nyquist frequency limit $\left(\frac{F_s}{2}\right)$ leading to aliasing problems during sampling at the receiver. A digital oversampling (interpolation) of the temporal sequence is then needed before DAC using e.g. zero-padded versions of the frequential sequences $S^m[k], k \in \{0,\dots,2K-1\}$.

2) Reception under FIR assumption: The voc signal delivered by the PV module is sampled by the oscilloscope at sampling frequency F_s. The whole sequence of received samples is then cut into M shorter sequences $y^m[n], n \in \{-L,\dots,2K-1\}, m \in \{1,\dots,M\}$ where the sequence corresponding to the $2K$ last samples of y^m (*i.e.* after CP cancellation) is synchronized to the corresponding s^m by correlation. Assuming a long enough CP duration, any sequence $y^m[n], n \in \{0,\dots,2K-1\}$ will be seen as a noisy linearly filtered version of one and the same OFDM symbol $s^m[n], n \in \{0,\dots,2K-1\}$:

$$y^m[n]=\sum_{l=0}^{L}h[l]s^m[n-l]+\eta^m[n],\ n\in\{0,\dots,2K-1\}, \quad (3)$$

where $\eta^m[n],\ n \in \{0,\dots,2K-1\}$, represents a noise sequence and where $h[l],\ l=0,\dots,L$ are the $L+1$ coefficients of a finite impulse response (FIR) filter. Such a linear filter is thus supposed to modelize the transfer of the overall LiFi system *i.e.* from the AFG voltage signal modulating the emitting LED light up to the voc signal provided by the PV module. Validity of such a model will be discussed later.
Let us introduce now $Y^m[k],\ k \in \{0,\dots,2K-1\}$, the DFT of the sequence $y^m[n],\ n \in \{0,\dots,2K-1\}$:

$$Y^m[k]=\sum_{n=0}^{2K-1}y^m[k]\exp\Big(-\mathrm{j}2\pi\frac{kn}{2K}\Big), \quad k\in\{0,\dots,2K-1\}.$$

Replacing $y^m[n]$ by (3), then $s^m[k]$ by (1) and taking into account the orthogonality property (2), the previous expression becomes

$$Y^m[k]=H[k]S^m[k]+N^m[k], \quad k\in\{0,\dots,2K-1\}, \quad (4)$$

where $H[k]=\sum_{l=0}^{L}h[l]\exp^{-\mathrm{j}2\pi\frac{kl}{2K}}$, $k \in \{0,\dots,2K-1\}$, is the assumed complex frequency response of the LiFi system for the frequencies $k\frac{F_s}{2K}$ and where the sequence $N^m[k],\ k \in \{0,\dots,2K-1\}$, is the DFT of the noise temporal sequence $\eta^m[n],\ n \in \{0,\dots,2K-1\}$.

C. LiFi performance frequency indicators

The proposed LiFi performance measurements are mainly based on the accurate estimation of the frequency response $H[k],\ k \in \{1,\dots,K-1\}$:

- *Frequency Response (Bode diagram):* From (4) and assuming that the noise is zero-mean, an unbiased estimate $\hat{H}[k],\ k \in \{1,\dots,K-1\}$ of the frequency response is obtained averaging over the M available sequences:

$$\hat{H}[k]=\frac{1}{M}\sum_{m=1}^{M}\frac{Y^m[k]}{S^m[k]}, \qquad k\in\{1,\dots,K-1\}. \quad (5)$$

  From the magnitude $|\hat{H}[k]|$, one can extract e.g. the cutoff frequency and the slope of the (low-pass) FIR-filter characterizing the on-test LiFi system.

- *Frequency SNR:* Replacing $H[k]$ by its estimate $\hat{H}[k]$ in (4), a noise estimation can be computed in the frequency domain, for each sequence m, using $Y^m[k]-\hat{H}[k]S^m[k]$, $k \in \{1,\dots,K-1\}$. It follows that the frequential distribution of the SNR at the LiFi system output can be estimated by

$$\mathrm{SNR}[k]=\frac{\sum_{m=1}^{M}\left|S^m[k]\right|^2}{\sum_{m=1}^{M}\left|Y^m[k]-\hat{H}[k]S^m[k]\right|^2}. \quad (6)$$
$$k\in\{1,\dots,K-1\}.$$

Naturally, these previous performance indicators are based on the assumption that the whole LiFi system is linear. We are aware that both the LED and the PV module may exhibits nonlinear behaviors and in practice, this assumption is often only partially satisfied.

- *Bit error rate:* When the linear assumption vanishes, the quality of the LiFi transmission can nevertheless be evaluated using the bit error rate. It is important to note that this indicator does not characterize the only LiFi hardware since it is also impacted by the chosen modulation scheme (here DCO-CP-OFDM).

III. Testbed validation

Here, 4-states constellations (4-QAM) modulate 127 carrier frequencies (taken between 39kHZ and 5MHz) to form a sequence of 346 OFDM symbols, with a 1/8 T_u cyclic prefix duration.

Fig.3 illustrates the magnitude frequency responses $|\hat{H}[k]|$ $(k = 2, \ldots, 128)$ estimated by averaging over the 346 OFDM symbols for both a photodetector Hamamatsu APD and a CIGS PV module made by AscentSolar, for different transmitter/receiver (T/R) distances *i.e.* different light expositions measured using a LX108 Light Meter from Française d'Instrumentation. It can be compared to Fig.4 summarizing the results obtained in [4] with the CEA-Leti LiFi testbed for close experimental conditions.

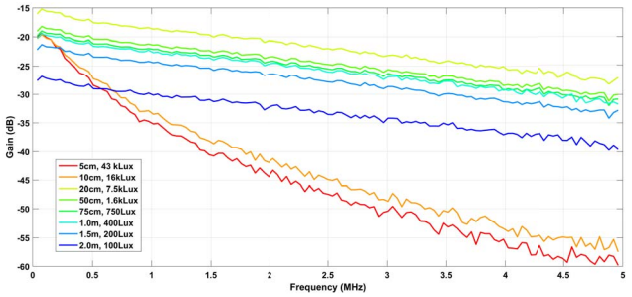

Fig. 3. Hamamatsu frequency responses from IM2NP testbed

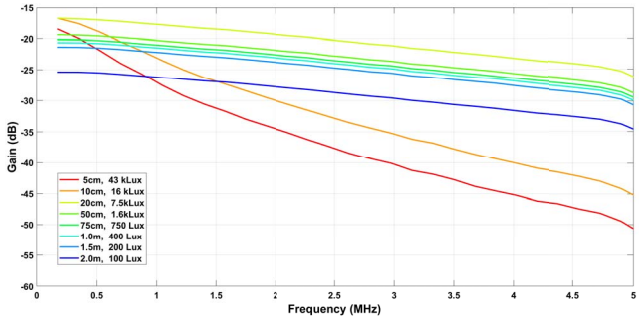

Fig. 4. Hamamatsu frequency responses from CEA-Leti testbed

These two figures show that the two testbeds exhibit similar results. Note that the smoothest effect on the CEA-Leti is due to an average over 4 scans. Generally, IM2NP's testbed find a higher attenuation. This phenomenon can be explained by some differences on devices used like a different LED's transfer function. Netherless, very similar variations with the T/R distance are observed in both figures.

The following Fig.5 and Fig.6 compare the results obtained from a CIGS PV module with the two testbeds in the same experimental conditions.

Again, one can note similar behaviors toward the T/R distance and the differences between the two CIGS responses can be explained by the aging of our CIGS PV module sample.

We can see by comparing Fig. 3 and Fig. 5 that for an illuminations higher than 16 kLux the Hamamatsu APD photodetector present a "saturation effect" and becomes less sensible than the CIGS PV module on this frequency range.

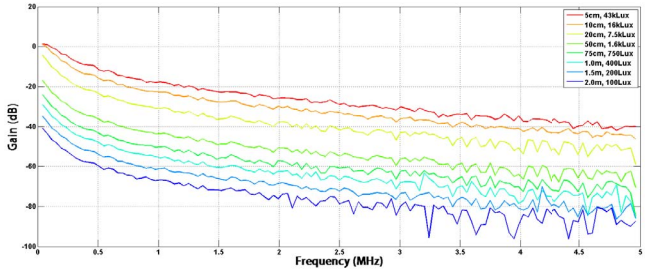

Fig. 5. CIGS PV module frequency responses from IM2NP testbed

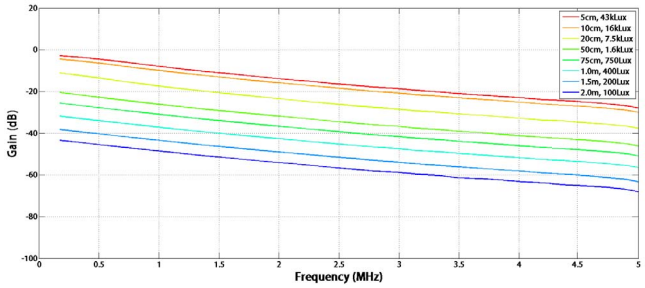

Fig. 6. CIGS PV module frequency responses from CEA-Leti testbed

IV. Results on semi-transparent PV modules

We give here results on 6 different a-Si semi-transparent PV modules shaped by Sunpartner.

A. LiFi test bench

The PV parameters of our different samples are given in Tab. I.

TABLE I
AM1.5 PV parameters of Sunpartner modules

Module	Characteristics					
	Techno	*Voc (V)*	*Isc (A)*	*FF*	*Rs (Ω)*	*Rsh (Ω)*
04-T1	a-Si	4.47	0.086	47.12	13.22	333.62
422-02-T4	a-Si	3.43	0.083	43.63	17.01	270.36
422-02-T3	a-Si	4.14	0.056	27.11	74.39	89.77
422-10-T3	a-Si	4.55	0.076	34.28	40.55	228.67
422-03-T2	a-Si	4.64	0.068	20.76	141.34	71.12
215-14-T3	a-Si	4.33	0.077	30.48	41.64	118.69

The LiFi test bench illumination conditions are:

- Software settings:
  - Modulation type: CP-DCO-OFDM
  - Oversampling: 10
  - Number of carriers: 127
  - Guard interval: 1
  - Constellation map: QPSK
  - Frequency range: 78 kHz $\rightarrow$ 2.4 MHz
- Hardware settings:

- LED: Philips Lumileds Luxeon CoB Core Range (Gen 3) L2C5-40901202E0900
- AC Generator: 10 Vpp
- DC Generator: 200 mA

A LiFi performance measurement of our 6 modules can be found in the Fig.7 for a 6000 lux illumination.

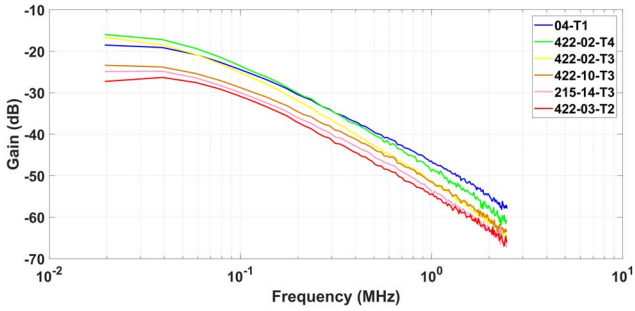

Fig. 7. Bode magnitude plot of the 6 modules

TABLE II
VOC AND SLOPE OF THE BODE MAGNITUDE PLOT

Module	*Open circuit voltage (V)*	*Slope (dB/dec)*
04-T1	2.48	-22.20
422-02-T4	1.00	-25.60
422-02-T3	2.55	-26.64
422-10-T3	3.78	-22.77
422-03-T2	3.30	-23.85
215-14-T3	4.12	-23.76

Except the behavior of modules 422-02-T4 and 422-02-T3, all modules have quite similar slopes (approximatively $-23dB/dec$ as seen in Tab. II) but they can not be interpreted as first or second order filter.
This means that here, the only parameter to drive LiFi performance is the magnitude voltage at low frequency.

As reported in Table II, we should also notice that our 6 modules do not exhibit the same Voc under LiFi illumination, in contrary to their behavior under AM1.5.

Such phenomena have still to be investigated.

V. CONCLUSION

In this article, we presented our functional LiFi testbed and validated it by comparison with that of CEA-Leti. A DCO-OFDM modulation scheme was chosen in order to characterize the system in the same conditions that those of a LiFi data transmission.
Very first results obtained from differents Sunpartner PV modules show that similar transfer functions can be observed. New investigations are needed to propose a filter model characterizing such semi-transparent PV modules.

REFERENCES

[1] E. Bialic, L. Maret, and D. Kténas, "Specific innovative semi-transparent solar cell for indoor and outdoor LiFi applications", Applied Optics, vol. 54 No. 27, pp. 8062–8069, September 2015.
[2] J. Armstrong, "OFDM for Optical Communications,"Journal of Lightwave Technology", vol. 7, No. 3, pp. 189–204, February 2009.
[3] L. Chassagne, "Technologie LiFi,"Techniques de l'ingénieur", TE7511 V1, pp 1–11, May 2017.
[4] R. W. Chang, "Orthogonal Frequency Multiplex Data Transmission System", U.S. Patent 3,488,445, 1966.
[5] "ETSI Standard : EN 300 744 V1.5.1 Digital Video Broadcasting" (DVB),
[6] R. Lassalle and M. Alard,"Principles of modulation and channel coding for digital broadcasting for mobile receivers", EBU Tech. Rev., pp. 168190, 1987.
[7] J. Armstrong,"OFDM: From copper and wireless to optical" presented at the Proc. OFC/NFOEC 2008, San Diego, CA, 2008, Tutorial, OMM1.
[8] N. Silsirivanich, D. Chenvidhya, K. Kirtikara, K. Sriprapha, J. Sritharathikhun, R. Songprakorp, and C. Jivacate, "Nonstationary effects at photovoltaic module characterization using pulsed solar simulator," Journal of Applied Spectroscopy, vol.82 No.2, pp. 286–292, May 2015.
[9] M. C. Di Piazza, A. Ragusa, M. Luna, and G. Vitale, "A Dynamic Model of a photovoltaic generator based on experimental data," International Conference on Renewable Energies and Power Quality, vol.1 No.8, pp. 1410–1416, April 2010.